Scalable methodology for the photovoltaic solar energy potential assessment based on available roof surface area: application to Piedmont Region (Italy)

Luca Bergamasco, Pietro Asinari

Department of Energetics, Politecnico di Torino,
Corso Duca degli Abruzzi 24, Torino, Italy

Abstract

During the last few years the photovoltaic energy market has seen an outstanding growth. According to the new Directive on renewable energies of the European Commission (2009/28/EC), the European Union should reach a 20% share of the total energy consumption from renewable sources by 2020. The national overall targets impose for Italy a 17% renewable share: in case of failure the gap would be filled by importation of renewable energy from non-UE countries. The abitious national targets and thus the continuously increasing interest on renewable fuels, require simple but reliable methods for the energy potential assessment over large-scale territories. Considering roof-top integrated PV systems, the assessment of the PV energy potential passes through the evaluation of the roof surface area available for installations. In the present paper a methodology for estimating the PV solar energy potential is presented, together with its application to Piedmont Region (North-Western Italy). The roof area suitable for solar applications, is calculated through the analysis of available GIS data. The solar radiation maps are taken from the database of the Joint Research Centre of the European Commission. Different solar energy exploitation scenarios are proposed with the relative perspective results and confidence interval. Further developments and applications of the presented methodology are finally discussed.

Keywords: Photovoltaic; Roof-top PV systems; Renewable Energy; GIS

Nomenclature

N	Number of	$[\,-\,]$
S	Surface	$[\,\mathrm{m}^2\,]$
P	Population	$[\,-\,]$
D	Density	$[\,\cdot/\mathrm{km}^2\,]$
C	Coefficient	$[\,-\,]$
η	Efficiency	$[\,-\,]$
μ	Exp. distribution rate parameter	$[\,-\,]$
H	Global solar irradiation	$[\,\mathrm{Wh/m}^2\,]$
T	Temperature	$[\,^\circ\mathrm{C}\,]$
Π	Electric energy potential	$[\,\mathrm{Wh}\,]$

Subscripts & Superscripts

inhab	Inhabitants
m	Mean
tot	Total
avail	Available
bui	Building
res	Resident, residential
ind	Industrial
mun	Municipality

pro	Province
pop	Population
mod	Module
amb	Ambient
MC	Mono-crystalline
PC	Poly-crystalline
TF	Thin Film

Abbreviations

GIS	Geographic Information System
BIPV	Building integrated PV system
EEA	European Environment Agency
CTRN	Numerical Technical Regional Map
VMAP	Vector Map
DEM	Digital Elevation Model
ESRA	European Solar Radiation Atlas
ISTAT	National Institute for Statistics
HVAC	Heating Ventil. and Air Cond. systems
STC	Standard Test Conditions
AM	Air mass coefficient

1. Introduction

The interest on renewable energies is growing day by day, as fossil fuels become always more expensive and difficult to find. Furthermore, the latest environmental disasters caused by the oil drilling and transportation, have further focused the attention of the entire world on the risks connected to fossil fuels. In the last April 2010, the explosion and sinking of the *Deepwater Horizon* oil rig in the Gulf of Mexico, and the start of the subsequent massive oil leak, is a clear example. During the last years, many attempts have been made to contain and control the scale of the environmental disasters, but the common sensation that fossil resources are "rapidly" going towards the end is widespreading. One of the most interesting, among the *"green resources"*, is the solar energy. The employment of the solar radiations has a wide range of applications, nevertheless the interest of solar engineering is mainly focused on thermal processes and photovoltaic applications. Particularly, taking into account the photovoltaic solar energy conversion, the building-integrated PV systems (BIPV) hold an important slice of the energy market (besides other common applications, i.e. *PV farms*). Integrated systems should be in general preferred to massive installations, for a rational use of the natural resources. In Italy, the continuous and uncontrolled installation of PV farms over the territory (highly profitable due to the economic incentives (Conto Energia 2010, [1])), is indeed jeopardizing the natural landscape and occupying more and more agricultural terrains. The increasing rate of these installations and the subsequent consequences are drawing the attention of the public opinion and are cause of alarm. In Italy, the large exploitation of the solar energy is at the beginning and actually there exist no regulation of the PV installations. The number of installations in Piedmont is growing insomuch as in July (2010) the Regional Council has approved a draft law to regulate the land use and to accommodate photovoltaic systems on the ground (Regional Council of Piedmont website [2]). This moratorium against the photovoltaic disfiguring, has been thought to either regulate the installations and promote the BIPV systems. The energy policy of the actual administration indeed foresees to motivate the installations on buildings or anyhow on already compromised marginal areas.

The incentive to the large scale utilization of building integrated modules however supposes the knowledge of the technical and economic territorial potential. Several works have been carried out on building integrated PV system installations (Castro et al. [3], Sorensen [4]), but generally the available roof surface area is assumed to
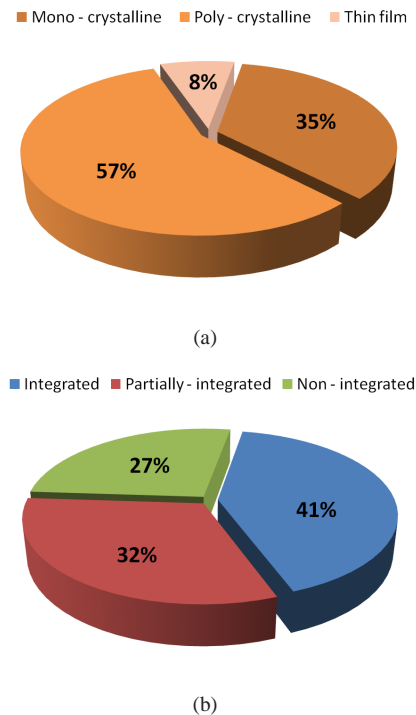

(a)

(b)

Figure 1: (color online) Subdivision of the electric power production [%] by different module technology (a) and different system-integration (b) over Piedmont Region in 2009 [10].

be an input. Furthermore, the detail of the available surface for PV installations is the *built-up area*, evaluated through maps of the land use (i.e. Corine Land Cover, of the European Environment Agency (EEA website [5])). This lack of methodology for the assessment of the available roof surface area, has been partially filled by some recent papers. A first scalable methodology for the roof surface assessment based on crossed-processing and sampling of various GIS data has been proposed together with its application to Spain in 2008 (Izquierdo et al. [6]). Very recent papers discuss similar methodologies and their relative applications to different geographical regions (Kabir et al. [7], Wiginton et al. [8]). The increasing literature on the topic reveals the growth of interest for the widespread exploitation of the solar power by means of building-integrated systems.

In Italy, in 2009, the total electrical energy consumption has been of about 320 TWh ([9],[10]), on the other hand the total production has been of about 275 TWh, corresponding to a 14% deficit ca. The paucity of the production has been balanced through importation from abroad. The Piedmont Region in 2009 has seen a production of 24.5 TWh ca. against a demand of 26 TWh

ca. (deficit of 6% ca.). Considering only the photovoltaic production, Piedmont produced 50.2 GWh, corresponding to 7.5% ca. of the total photovoltaic production in Italy. The energy production is subdivided on different module technologies and different kind of installations/integration[1] (Fig. 1(a), 1(b)). It is important to notice that in Piedmont, the number of installations and the installed power in 2009 has been more than twice that of 2008 (respectively +118% and +149%), [10].

The present paper deals with the PV solar potential assessment over the Piedmont region through the evaluation of the roof surface available for grid connected building-integrated PV installations (BIPV). For the sake of clearness, we remind that the term BIPV generally refers to either roofs and façades, in the paper we use it to refer to roof-top integrated PV systems only. The work is organized as follows: the general outlines of the methodology are first presented. Subsequently, the procedure for the assessment is discussed in detail together with the various data processing. The results are presented progressively: from the municipal to the regional scale. Different scenarios for the solar energy exploitation are presented together with their confidence interval and finally, the conclusions on the present work are drawn and perspective developments of the methodology are proposed.

2. Methodology

The assessment of the photovoltaic solar energy potential requires the evaluation of the *physical potential* (useful solar radiation), *geographical potential* (roof surface available) and *technical potential* (PV system efficiency). The estimated theoretical PV potential is achieved proceeding through a hierarchical assessment methodology (Fig. 2). Generally, in large scale analysis like this, a certain level of approximation has always to be accepted, thus the effort is to be done to contain the errors as much as possible, in order to achieve reliable results. The evaluation of the various potentials requires to take into account a wide range of different parameters. In the present study, it has been decided to counter the risk of misleading results evaluating different scenarios for each uncertainty, in a sort of parametrical study. The initial stage of the analysis, corre-

---

[1]The level of integration of the PV modules is generally referred to three main typologies: *non-integrated*, for ground-mounted systems (i.e. PV farms), *partially-integrated* if the systems are installed on buildings by means of additional structures, *integrated* if the modules are intalled directly on building features (i.e. roofs, façades).
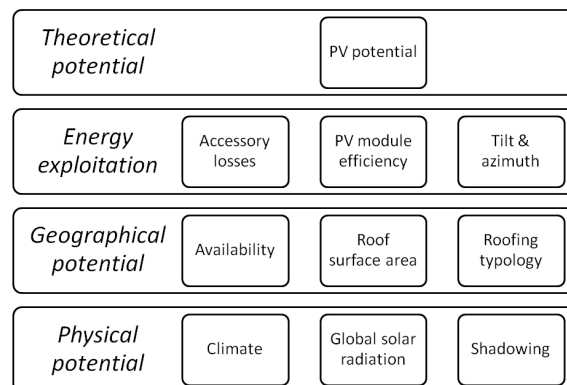

Figure 2: Scheme of the hierarchical methodology: the assessment foresees the estimation of the physical, geographical and technical potential (energy exploitation). The theoretical PV potential is achieved aggregating the data obtained through the various levels.

sponding to the collection of the various data is of fundamental importance as the accuracy of the final results depends in great measure on the precision of the original data (as well as on the accuracy of the analysis and on the number of affecting parameters taken into account). A review of the available data necessary for the analysis has allowed an overview on the maximum precision achievable and on the sources of the various data types. As regards the solar radiation data, it has been decided to refer to the maps provided by the Joint Research Centre of the European Commission, [17] (freely available for public use). The geographical and cadastral analysis relys on the Numerical Technical Regional Map of Piedmont CTRN (Carta Tecnica Regionale Numerica). The update of the sections of the map is different over the region, the newest (current) version presents updates from 1991 to 2005, but this is actually the most precise territorial data available and suitable for a large scale processing. For the sake of clarity, it has to be told that in Italy, all the cadastral data are held at the municipal level by the local cadastres. There have not been unification of the cadastral data at higher level until now and furthermore, all the data have not been computerized yet. There are nevertheless some projects, currently ongoing, aiming to digitalize and associate the cadastral data to the numerical maps. Such a document would allow the possibility to have all the cadastral informations associated to the entities present in the numerical maps (i.e. height of buildings, number of resident persons per building, etc.).

All the analysis on the maps are performed in a commer-

cial GIS software, ESRI ArcGIS 9.3. The data is successively exported for the processing, which has been performed in MATLAB.

2.1. Solar radiation data

The solar radiation maps for Europe are freely available on the website of the Joint Research Centre (JRC) of the European Commission, [17]. The solar radiation database has been developed from the climatologic data available in the *European Solar Radiation Atlas, ESRA* (ESRA website [16]), homogenized for Europe. The algorithm used to build the database, accounts for beam, diffuse and reflected components of solar irradiation. Basically, the irradiation is computed by integration of the irradiance values measured at imposed time intervals during the day. For each time interval the effect of sky obstruction (shadowing by local terrain features) is computed by means of the Digital Elevation Model (DEM). For the sake of completeness, the calculation steps in the construction of the model are briefly reported hereafter, for the details on the algorithm refer to M. Šúri et al. ([11]), M. Šúri and Hofierka ([12]), M. Šúri et al. ([13]). The model has been developed through the following steps:

1. computation of clear-sky global irradiation on a horizontal surface;
2. calculation and spatial interpolation of clear-sky index and computation of raster maps of global irradiation on a horizontal surface;
3. computation of the diffuse and beam components of overcast global irradiation and raster maps of global irradiation on inclined surfaces;
4. accuracy assessment and comparison with *ESRA* interpolated maps.

On the website it is also possible to interrogate an interactive tool, the Photovoltaic Geographical Information System (PVGIS), and to obtain the solar radiation (kWh/m^2) and the photovoltaic electricity potential (kWh) in a certain location (and for an assigned installed peak power), calculated on the basis of the desired parameters (i.e. module technology, mounting options, tracking options, etc.). The utility provides daily and monthly mean values and the yearly sum. The database has already been used to analyse regional and national solar energy resource and to assess the photovoltaic (PV) potential in European Union member states (Marcel Šúri et al., [14]). For the purpose of the present study, in order to obtain the solar radiation data at the municipal detail, the raster maps are the most suitable tool. Among the available maps on the website, the following are taken into account in the present paper:
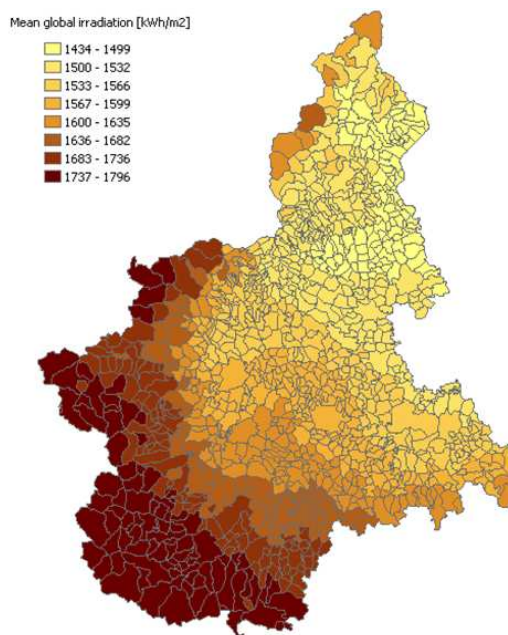

Figure 3: (color online) Yearly sum of global irradiation on the Piedmont region [kWh/m^2]. The colors refer to the mean global radiation per municipality. These values are the interpolated among all the cell-values of the solar radiation map falling within the municipality.

- yearly sum of global irradiation on optimally-inclined surface (kWh/m^2);
- optimum inclination angle of equator-facing PV modules to maximise yearly energy yields (°).

The raster maps are in format ESRI ascii grid, and the original map projection is geographic, ellipsoid WGS84. The rasters cover the extent within the following bounds: North 72° N, South 32°30' N, West 27° W, East 45° E. Each map consists of 474 rows and 864 columns, for a total of 409536 cells. The grid cell size has a resolution of 5 arc-minutes (corresponding to 0.083333°), obtained aggregating the original data with 1 km resolution. All the raster maps have been vectorized, overlayed to the Piedmont numerical map and clipped by the regional borders (Fig. 3). Each data layer (solar radiation and optimum inclination angles) has been joined to the Piedmont vector map assigning to each municipality the corresponding property. Particularly, the interpolated value of the pixels within the municipality is taken.

2.2. Territorial analysis

The CTRN of the Piedmont Region is a vector map (*VMAP*), consisting of 70 *"sheets"* in scale 1:50000 ob-

Figure 4: (color online) Comparison of the Piedmont numerical map (a) with the *Google Earth*™ image (b) for the same location. The snapshots show a view of Politecnico di Torino and neighborhood. In the view from the numerical map (a) it is possible to see the edge where two sections have been merged.

tained from the digitalization of the original CTR paper map and geo-referenced in WGS84/UTM (ellipsoid/projection type). Each sheet is divided into 16 *"sections"* in scale 1:10000, for a total of 1120 sections. The sections are distributed in the form of compressed archives, for a total data size of 21 GB ca. (subdivided in 45 CD-roms). The formats available are: *e00* format, an ESRI proprietary format to be used by means of GIS sofware, *dxf* format for AutoDesk, ESRI *shape3D* (this last only for the Dora river basin, until now). In the present work the *e00* format is used. All the 3191 *e00* files have been filtered and extracted from the CD-roms for the processing, the actual size of the compressed data is 9.6 GB ca. All files have been extracted to *coverages*. The coverage is a file containing multiple sub-files for points, lines and polygons. The sub-files have been filtered and, for our purpose, only those containing polygons have been selected. These files have then been converted to the most common *shp* file-type. This latter format, the *shapefile* is a *meta-data* format, which is able to store multiple informations for the same object. It is organized into geometries, which are geo-referenced polygons called *entities*. Each entity corresponds to an object, such as buildings, roads, rivers, etc. Each polygon stores a certain quantity of available informations, as for example its area and perimeter or its intended use. The storage of informations is achieved by means of at least three interconnected files (in this case there is a fourth optional file):

- *shp* file, geometries;
- *shx* file, indexes of the geometries;

- *dbf* file, attribute database;
- *prj* file, reference system (optional).

The *shp* files have then been merged and organized in a *file geodatabase*, a new ESRI compressed database format for large scale analysis. The data size at this point is 4 GB ca. Now it is possible to work and perform the analysis on the shapefiles of the entire region. The map can be directly interrogated and several studies can be performed. It is possible to filter or select entities by attributes or intended use, for instance. The strategy of the present study is to assess the roof surface area available for intallations per municipality. The municipality is indeed considered the smallest unity for the analysis. In order to associate each polygon to its administrative domain, a new shapefile containing the polygons representing the administrative limits of the municipalities has been layed upon the Regional map (obviously according to the same geo-referenced coordinate system and projections). In this way it has been possible to associate each entity of the CTRN to the municipality it belongs to. The association has been performed on the basis of the spatial location of the polygons. The criteria foresees that a polygon is associated to the relative municipality only if it falls completely inside. If a polygon falls in more than one administrative limit, the polygon is associated to the first municipality encountered by the algorithm. Another possible criteria could have been to associate a polygon to the municipality where the most of the area falls into. In both cases an error occurs, because it should be kept in mind that:

- the shape of the polygons representing the administrative limits is slightly simplified;

- an ambiguous building (falling on the administrative limit), in the reality, is not necessarily assigned to a certain municipality only on the basis of its spatial location;

- the obtained data cannot be verified, as neither the local administrations nor the cadastre, systematically provide this kind of informations.

The entity of the error due to the association algorithm will be discussed in the section dedicated to the methodologic uncertainties. After the association of the polygons to the municipalities, the entities have been filtered to calculate the number of residential and industrial buildings per municipality and the total roof surface area available. For the sake of clarity, a brief clarification on the use of the term "building" is mandatory: in the paper this term refers to a polygon characterized by a certain intended use (i.e. single or groups of adjacent residential or industrial structures).
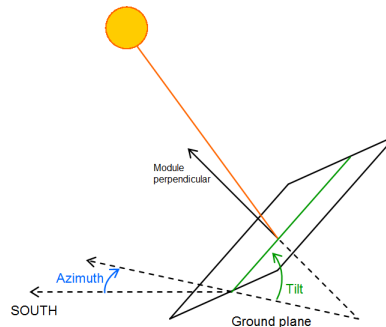
2.3. Residential and industrial roofing

The total roof surface area computed in the previous section, relys on the complete cartographical dataset of the entire region, namely it can be assumed to be errorless. The evaluation of its effective available share however, requires the introduction of empirically found cutting coefficients. The lack of informations on the roofing properties indeed, imposes the assumption of a representative roofing typology and its empirical analysis based on the visual inspection of *Google Earth™* images. In the following paragraphs the residential and industrial roofings are treated separately.

2.3.1. Residential

In Italy, especially in the north, the most employed roof typology is the double-pitched (in the southern regions flat roofs are also common). Here we assume that the representative residential roofing typology over the Piedmont Region is double-pitched (Fig. 5(a)). The slope of the pitch is usually calculated according to the maximum theoretical snow-load (besides the roofing material). The slope of the roofs is indeed steeper in the mountains. In Piedmont the slope of the pitches can be assumed to range between 30 and 45% (17 to 24° ca.). This consideration allow to calculate the effective roof surface area. It should indeed be noticed that the building areas extrapolated from the CTRN are the 2D projections of the real roof surface. These areas are
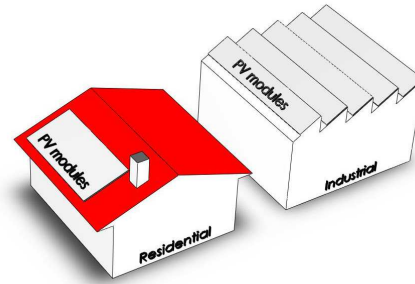
(a)

(b)

Figure 5: Schematic example of the representative roof typologies for residential and industrial buildings in Piedmont with roof-top integrated PV installations (a). Definition of the *tilt* and *azimuth* angles for PV applications (b).

hence supposed to be corrected by their own slope. We assume a characteristic inclination angle for residential roofing of 20° ($\theta_{res} = 20°$), and correct the area by a $cos(\theta_{res})$ factor.

In the present paper it has been also decided to consider the installation of the modules only on one of the two pitches of each roof (typically the best exposed to the sunlight), which is the most common solution adopted. This consideration leads to decrease the roof surface available per building of 50% (*roof-type coefficient* $C_{RT} = 0.5$). Furthermore the roof surface available for installations has been considered to be 70% of the total pitch, considering the space already occupied by chimneys, aerials or windows (corrective *feature coefficient* $C_F = 0.7$). Precautionary we consider also that a 10% of the roof surface may not be available because already occupied by solar-thermal systems (corrective *solar-thermal coefficient* $C_{ST} = 0.9$). Another mandatory consideration on the roof area exploitation involves the reciprocal shadowing of the PV module series. In order to avoid the undesirable reciprocal shadowing, a

6

Table 1: Summary table of the coefficients and angles of eq. (1). *Roof-type coefficient C_{RT}, feature coefficient C_F, solar-thermal coefficient C_{ST}, covering index coefficient C_{COV}, shadowing coefficient C_{SH}, total corrective coefficient C_{TOT}. The pitch inclination angle θ is 20°* for residential and 30° for industrial roofing.

Coefficient	Residential	Industrial
C_{RT}	0.500	0.750
C_F	0.700	0.900
C_{ST}	0.900	1.000
C_{COV}	0.450	0.450
C_{SH}	0.460	1.000
C_{TOT}	0.065	0.304

sufficient gap must be provided among the panels. In order to take into account these gaps, we introduce the *covering index coefficient $C_{COV} = 0.45$*, which represent the ratio of module surface divided by the total roof surface available (Lorenzo et al., [15]). The last consideration to be done on the roof surface availability concerns the shadowing produced by other buildings or by the roof itself. The computation of this coefficient would require a 3D city model, namely at least the height of buildings. Despite some projects, currently ongoing, aim to construct such a model for the Piedmont region, at today this kind of data is not available. Having no other informations about the reciprocal shadowing of buildings, we assume for this coefficient the value found by Izquierdo et al., [6], for our representative building typology (RBT), which is 0.46 (*shadowing coefficient $C_{SH} = 0.46$*).
Considering all the above coefficients, their product yields the total corrective coefficient C_{TOT} (Tab. 1). The roof surface available is finally calculated by the following equation (1):

$$S_{roof}^{avail} = C_{RT} \cdot C_F \cdot C_{ST} \cdot C_{COV} \cdot C_{SH} \cdot \frac{S_{roof}}{cos(\theta_{res})} \quad (1)$$

2.3.2. Industrial

The industrial roofing is generally different from that of residential buildings. Despite the roof surface available can still be evaluated by means of equation (1), the different typology impose different values of the corrective coefficients and inclination angle. In particular, we consider that the most common roof typology for industrial applications is the pitched-roofing (Fig. 5(a)), which is perfectly suitable for integrated PV installations. The *roof-type coefficient C_{RT}* is in this case as-

sumed to be 0.75 (considering a 25% of the roof without sheds), the *feature coefficient C_F* equal to 0.9 (for chimneys or HVAC systems) and *solar-thermal coefficient C_{ST} = 1* (generally industrial roofing is not used for solar-thermal systems). The characteristic shed inclination angle is assumed to be 30° (θ_{ind} = 30°). The integrated system should again be installed by means of proper supports to achieve the optimal tilt angle. The covering index coefficient is equal to 0.45, considering the module series on a single shed and the shadowing coefficient is equal to 1, as industrial buildings are generally isolated. A summary of the parameters used in eq. (1) for the residential and industrial roofing is reported in Tab. (1).
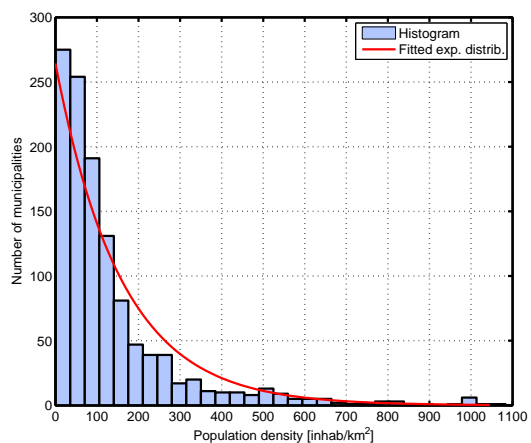
Figure 6: Histogram and fitted exponential distribution of the population density. The mean value is 158 inhab/km^2 (μ = 158 $inhab/km^2$), the maximum is Torino with 6982 inhab/km^2 (cut-off point of the x axis at 1100 inhab/km^2). It is noticeable the strong dispersion of the population. This is mostly due to the scarcely populated montain regions.

2.4. Population

All the data concerning the population have been taken on the website of the National Institute for Statistics IS-TAT, [18]. Particularly the list of all the Italian municipalities is freely available on the website [19]. The data-sheet provides informations on each municipality: name, ISTAT code, number of resident population and the province each municipality belongs to. The Piedmont Region (total population of 4432571 inhabitants) is divided into 1206 municipalities, organized in 8 provinces: Torino (TO), Vercelli (VC), Novara (NO), Cuneo (CN), Asti (AT), Alessandria (AL), Verbano-Cusio-Ossola (VB) and Biella (BI). A first interesting consideration on the population distribution can be

drawn: 50% ca. of the total number of municipalities counts less than 1000 inhabitants. The municipalities with more than 50000 inhabitants are only 8, and 1 over 150000 (Torino, with 910000 inhabitants ca.). The mean population density is 158 inhabitants per km^2, the maximum belongs to Torino, with 6982 inhabitants per km^2. It is noticeable that the Piedmont region is characterized by a very high concentration of the population in the main cities (Torino by far over the others). The region presents a strong dispersion of population outside the main cities. This disparity is mostly due to a high number of municipalities located in the mountain region of the Alps which are scarcely populated. Fig. 6 show the histogram and fitted exponential distribution of the population density over the region. For the sake of clarity, we briefly remind the definition of the pdf (probability density function) of an exponential distribution for a sample x (eq. 2):

$$f(x \mid \mu) = \frac{1}{\mu} \cdot e^{-\frac{x}{\mu}} \tag{2}$$

2.5. Energy conversion

At today, the most employed low concentrated PV module technologies are essentially three: *mono-crystalline (single-crystalline)*, *poly-crystalline (multi-crystalline)* silicon and *thin film (amorphous silicon)*. The mono-crystalline silicon is the oldest and more expensive production technique, but it is actually the most efficient sunlight conversion technology available. The poly-crystalline has a slightly lower conversion efficiency compared to the mono-crystalline, but the manifacturing costs are also lower. The thin film is obtained by vaporization and deposition of the silicon on glass or stainless steel. The production cost of this last technology is lower than any other method, but the conversion efficiency is also low. Generally the PV module manifacturers provide the *nominal peak power* at *Standard Test Conditions* (STC), which means at 1000 W/m^2 solar irradiance, a module temperature of 25°C ($T_{mod} = 25°C$) and with an air mass 1.5 (AM1.5)[2] spectrum. At today, the PV module market is extremely dynamic, there is a wide range of technologies (continuously changing) and a multiplicity of declared efficiencies by manifacturers for the various module typologies. For the purpose of the present study, it has been decided to assume the following representative values: mono-crystalline $\eta_{MC} =$ 15%, poly-crystalline $\eta_{PC} = 12\%$ and thin film $\eta_{TF} =$ 6%. It is well known that the efficiency depends on

---

[2]The air mass coefficient characterizes the solar spectrum after the solar radiation has traveled through the atmosphere.

several factors, such as operating temperature and irradiance. The module temperature in turn should be evaluated considering the ambient temperature, eventual cooling effect of the wind, etc. The evaluation of PV module losses (in no STC) is currently subject of great interest by the technical community, several papers are based this (i.e. E. Skoplaki, J.A. Palyvos [20], T. Huld et al. [21]). The performance of the modules, moreover, undergoes a decrease during the operating years (A.J. Carr, T.L. Pryor [22]).

In the present paper we neglect the efficiency worsening along the module lifetime and assume the losses due to temperature variations and irradiance to be 10% ($\eta_{TH} = 0.9$) for all the module technologies. As regards the conversion efficiency, two further important parameters must be taken into account: the module installation angles. If we assume that, given the slope of the pitched-roof, the fixed installation is realized so that the best inclination angle, or *tilt angle* (angle of inclination of the array from horizontal, 0° = horizontal, 90° = vertical, Fig. 5(b)) is achieved (by means of apposite supports), the solar radiation exploitation is maximized. It should be reminded that an increased tilt will favour the power output in the winter months, which is often desired for solar water heating instead, and a decreased tilt will favor power output in summer months. The optimal installation angle is a mean value, calculated to maximize the yearly energy yield. Another key factor to take into account in order to get the highest energy production from a photovoltaic system within a set geographic area has to do with maximizing the exposure to direct sunlight. It is necessary to avoid shade and expose the modules towards the sun, therefore realizing the module installation according to the best *azimuth angle* (angle of the panel with respect to the south, 0° = South, Fig. 5(b)). Considering fixed mounted, integrated PV systems, the installation azimuth should be that of the longitudinal roof axis, which is randomly different from the best (towards the south). In order to evaluate the losses due to the incorrect azimuth angle of the installation, the roof axes should be known. The territorial/cadastral data available at today, do not provide this kind of information. In order to overcome the problem, a corrective coefficient has been introduced, the *azimuthal efficiency, η_{AZ}*. For the given tilt angle, the value of this coefficient varies from 1 for south-facing PV modules to 0.9 for azimuth angles ranging between ± 90° (UNI 10349, [23]), namely we assume for this coefficient a value of 0.9 ($\eta_{AZ} = 0.9$). Besides all the above mentioned losses, other accessory losses must be taken into account for grid-connected PV systems. Hereby we consider the accessory losses as follows: 3% due to

Table 2: Summary table of the efficiencies for the various module technologies: MC mono-crystalline, PC poly-crystalline Silicon and TF thin film. Module efficiency η_{mod}, atmospheric efficiency η_{TH}, azimuthal efficiency η_{AZ}, installation efficiency η_{inst} and total system efficiency η_{TOT}.

η	MC	PC	TF
η_{mod}	0.150	0.120	0.060
η_{TH}	0.900	0.900	0.900
η_{AZ}	0.900	0.900	0.900
η_{inst}	0.840	0.840	0.840
η_{TOT}	0.102	0.081	0.041

Figure 7: Net electrical energy consumption [GWh] for province in 2009: Alessandria (AL), Asti (AT), Biella (BI), Cuneo (CN), Novara (NO), Torino (TO), Verbano-Cusio-Ossola (VB), Vercelli (VC)

reflection of the sunbeams of the array, 1% due to possible dirt or dust on the PV array, 2% due to the DC electric panel, 10% due to the inverter efficiency, for a total installation loss of 16% ($\eta_{inst} = 0.84\%$). Considering all the above efficiencies, their product leads to the total system efficiency per technology (η_{TOT}) (Tab. 2). The PV potential Π is finally calculated by means of the following equation (3):

$$\Pi = \eta_{mod} \cdot \eta_{TH} \cdot \eta_{AZ} \cdot \eta_{inst} \cdot H_m^{mun} \cdot S_{roof}^{avail} \qquad (3)$$

The distribution of the PV module typologies over the Region has been evaluated on the basis of the statistical data of 2009, [10]. The first possible scenario is to consider that in 2010, the total number of available roof surface area would be exploited by different module technology according to the statistical trend of 2009 (Fig. 1(b)). Two alternative scenarios are presented: the cases in which the energy would be exploited by means of the modules with the highest and lowest efficiency.

- scenario A, different module technologies;

- scenario B, mono-crystalline only;

- scenario C, thin-film only.

2.6. Electrical energy demand

The electrical energy demand has been evaluated by means of the public statistical data of 2009 available on the distributor website, [9]. The maximum level of resolution of the available data is the provincial detail. In 2009 the total net electrical energy consumption, that is excluding the electricity used for railway transports, has been of 24560.3 GWh for the whole region, namely 5532 kWh per inhabitant ca. The losses

have been of 1293 GWh increasing the total energy demand to 25853.3 GWh. Torino (TO) is by far the province with the highest consumption (10500 GWh), it required more than twice the energy needed by the second province with the highest consumption, which is Cuneo (CN) with 4403.5 GWh (Fig. 7). In 2009, the total net production of the entire region has been 24399.7 GWh, of which 66 % ca. from thermoelectric sources, 33.7 % ca. from hydroelectric and a negligible part from photovoltaic (0.2 % ca.) and eolic (0.07 % ca.) sources.

3. Results

The analysis has been carried out according to a hierarchical procedure, proceeding from the smallest unity (municipality) towards the regional scale. The presentation of the results follows the same order in the paper.

3.1. Municipal level

The large amount of data of the municipal detail, does not allow the presentation of the results achieved for the whole 1206 municipalities. The population has been thus divided into classes, according to seven quantiles (Tab. 3). It has been decided to report the numerical results for class 4 (number of inhabitants greater than 5000), which include 134 municipalities and describes 70% ca. of the population. Attached to the present work, the table in Appendix (Tab. 5) reports the numerical results achieved for the municipalities of this last class. The analysis has been nevertheless carried out on all 1206 municipalities. The total number of industrial and residential buildings per municipality has been

Table 3: Subdivision of the municipalities in classes according to the number of inhabitants. Seven quantiles have been used and it has been decided to report in Appendix (Tab. 5) the numerical results for class 4, describing 70% ca. of the whole population.

| Class	range	N_{mun}	$\%_{mun}$	Pop	$\%_{pop}$
1	≥1000	606	50	4145756	93.5
2	≥2000	353	29	3786720	85.4
3	≥3000	239	20	3516313	79.3
4	≥5000	134	11	3113066	70.2
5	≥10000	67	5.5	2631635	59.3
6	≥20000	32	2.5	2141437	48.3
7	≥50000	8	0.5	1394477	31.5

calculated, together with the relative available roof surface area (eq. 1). An example of the residential and industrial roof surface distribution achieved is reported for the municipality of Torino in Fig. 8(a) and 8(b) respectively. At this level, the results achieved on the PV potential are reported only for the exploitation scenario A (roof surface available divided in each municipality as follows: 35% mono-crystalline, 57% poly-crystalline and 8% thin film modules). The PV potential has been calculated for the residential only and industrial roofing only (eq. 1, 3), the total potential has then been achieved (Tab. 5 for municipalities of class 4, Fig. 9 for an overview of the whole region). The yearly sum of the global solar radiation over the region ranges between 1796 and 1434 $kWh/m^2 year$, with a mean value of 1560 $kWh/m^2 year$. It should be reminded that these values have been calculated assuming all the PV modules installed at the optimal inclination angle. For Piedmont, the mean optimal installation angle is 37° ca. (ranging between 35 and 40°). Despite the highest values of solar radiation are located on the mountain regions (Fig. 3), the low building density and thus the paucity of available roof surface area for installations, do not allow a full exploitation of the highest solar potential as shown in the next paragraph, *Provincial level*.

3.2. Provincial level

The results reported in this section are the aggregated of the municipal detail. The results achieved at the provincial level are reported in Tab. 4. The table is organized in sections and reports: general results for each province (population and number of municipalities), the results on the available residential and industrial roofing and the numerical results achieved for exploitation scenario
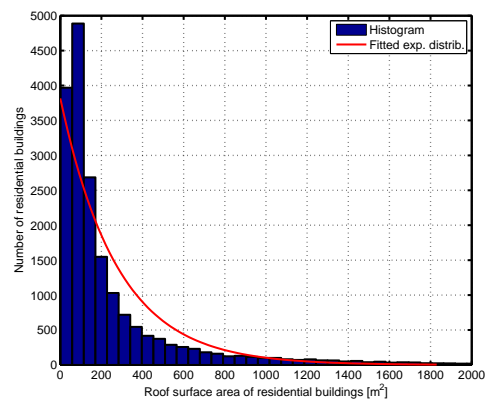
(a)
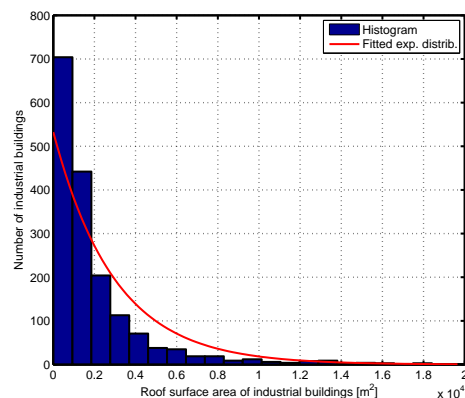
(b)

Figure 8: Histogram and fitted exponential distribution of the residential (a) and industrial (b) roof surface area in the municipality of Turin. For a better visualization, the cut-off points of the x axes are respectively 2000 and 20000 m^2. $\mu_{res} = 277\ m^2$ and $\mu_{ind} = 2974\ m^2$.

Table 4: Summary table for provinces: Population (P_{pro}), number of municipalities (N_{pro}^{mun}), population density (D_{pro}^{pop}) [$inhab/km^2$], number of residential buildings (N_{res}^{bui}), residential building density (D_{res}^{bui}) [bui/km^2], residential roof surface available (S_{res}^{avail}) [km^2], number of industrial buildings (N_{ind}^{bui}), industrial building density (D_{ind}^{bui}) [bui/km^2], industrial roof surface available (S_{ind}^{avail}) [km^2], mean solar radiation (H_m) [kWh/m^2year], PV potential for scenario A (res, ind, tot), (Π_A) [$GWh/year$].

	General			Residential			Industrial			Potential			
	P_{pro}	N_{pro}^{mun}	D_{pro}^{pop}	N_{res}^{bui}	D_{res}^{bui}	S_{res}^{avail}	N_{ind}^{bui}	D_{ind}^{bui}	S_{ind}^{avail}	H_m	Π_A^{res}	Π_A^{ind}	Π_A^{tot}
	[−]	[−]	$\left[\frac{inhab}{km^2}\right]$	[−]	$\left[\frac{bui}{km^2}\right]$	$\left[km^2\right]$	[−]	$\left[\frac{bui}{km^2}\right]$	$\left[km^2\right]$	$\left[\frac{kWh}{m^2year}\right]$	$\left[\frac{GWh}{year}\right]$	$\left[\frac{GWh}{year}\right]$	$\left[\frac{GWh}{year}\right]$
TO	2290990	315	335	311908	45	6.93	14435	2.10	10.92	1610	947	1478	2425
VC	180111	86	86	45138	22	1.07	1988	0.95	1.32	1519	140	172	312
NO	366479	88	274	66878	50	1.51	3294	2.46	2.08	1493	193	267	460
CN	586020	250	85	176291	26	3.90	5265	0.76	3.36	1696	566	484	1050
AT	220156	118	146	66965	44	1.39	3448	2.28	1.55	1588	189	211	400
AL	438726	190	123	115187	32	2.57	3328	0.93	2.28	1563	342	302	644
VB	162775	77	72	65085	29	0.81	1027	0.45	0.58	1499	103	74	177
BI	187314	82	206	45107	49	0.83	2357	2.57	1.69	1508	107	217	324
REG.	4432571	1206	174	892559	35	19.01	35142	1.38	23.78	1560	2587	3205	5792
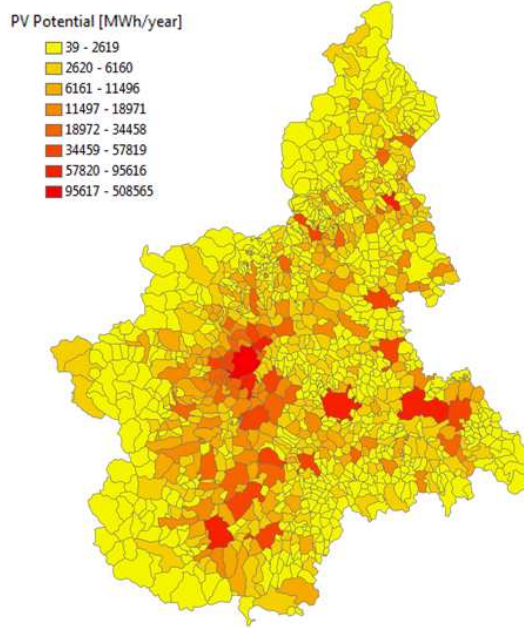
Figure 9: (color online) PV potential for each of the 1206 municipalities of the Piedmont Region (exploitation scenario A) [MWh/year].

A. The provinces with the highest mean solar radiation are Cuneo (CN) with 1696 kWh/m^2year, Torino (TO) 1610 kWh/m^2year and Asti (AT) 1588 kWh/m^2year. Despite Cuneo is the province with the highest mean solar radiation, the highest PV potential belongs to Torino (TO) (followed by Cuneo (CN) and Alessandria (AL)), because of the larger roof surface available. The employment of the industrial roof surface area accounts respectively for 61% (TO), 46% (CN) and 47% (AL) ca. of the total PV potential of the province. The exploitation scenario A is then compared with scenario B and C for each province (Fig. 10). Scenario B corresponds to energy exploitation by means of mono-crystalline modules only (highest efficiency, most expensive technology), an thus to the highest PV potential. Scenario C for thin film modules only (cheapest technology but lowest efficiency), and thus to the lowest PV potential. Comparing the PV potential for the three scenarios with the yearly electrical energy consumption shows that, despite none of the provinces would be able to sulf-sustain its local demand, the distributed PV energy production would cover a non-trivial share of the demand (between 20 and 40%). In particular, the province that would better benefit of the installations is Asti (AT), whose ratio of potential to the local consumption reaches nearly 50% (for the best exploitation scenario B) (Fig. 11).

3.3. Regional level

In this paragraph the aggregated results of the previous levels are reported. Over the entire region, the residential roof surface available for installations is 19 km^2 ca. and the industrial 24 km^2 ca., for a total of 43 km^2 ca. of roof top surface area suitable for BIPV installations.

Figure 10: (color online) Comparison of the yearly PV potential for the different exploitation scenarios (A, B, C) for the 8 provinces of Piedmont: Alessandria (AL), Asti (AT), Biella (BI), Cuneo (CN), Novara (NO), Torino (TO), Verbano-Cusio-Ossola (VB), Vercelli (VC).
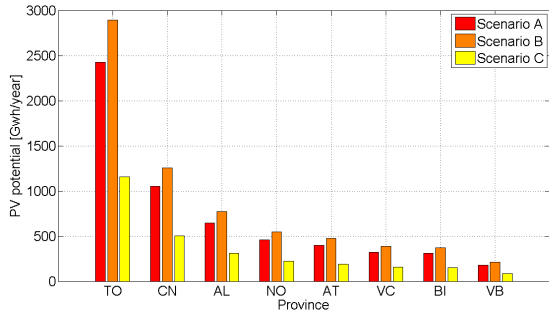

Figure 11: Electrical energy balance for the 8 provinces. The central line refers to the comparison demand/supply for scenario A. The error bars show the comparison of demand with scenario B (upper bound) and C (lower bound).

It is interesting to highlight that the industrial roofing accounts for a 56% ca. of the total roof surface available. Considering the total roof surface, the total PV potential achieved for scenario A is 5.8 TWh/year (2.6 TWh/year from residential and 3.2 TWh/year from industrial installations). On the other hand, according to scenario B, the total PV potential is 6.9 TWh/year (3.1 TWh/year from residential and 3.8 TWh/year from industrial installations), and 2.8 TWh/year for scenario C (1.3 TWh/year from residential and 1.5 TWh/year from industrial installations). According to the methodology proposed in the present paper, the yearly PV potential over the region for the proposed exploitation scenarios ranges between 2.8 and 6.9 TWh/year, which yields a total mean PV potential pro capite ranging between 632 and 1557 kWh/year. Considering only the residential buildings, the mean roof surface available pro capite is 4.3 m^2, for a PV potential ranging between 278 and 697 kWh/year. The yearly PV energy yield per square meter of installation is 135, 161 and 65 kWh/m^2year ca. for scenarios A, B, C respectively. Considering the yearly energy yield range per square meter, one may easily estimate his own PV production range simply multiplying these values for his meters of installation. In conlusion, it is interesting to make a comparison between the results obtained for Piedmont and the whole Italian energy production from PV resources in 2009 [9]: the total national production has been of about 676 GWh, Piedmont accounted for 50.2 GWh (7.5% ca.). The estimated total PV potentials for Piedmont range in three orders of magnitude above.

4. Confidence level

A systematical analysis over large-scale territories like this, is always affected by a certain level of uncertainty. Particularly, the accuracy of the final results strongly depends on the quality of the input data. The first uncertainty to consider is that the CTRN of the Piedmont region consists of various differently updated sections. The newest version presents updates from 1991 to 2005. The newly-built buildings, for instance, are not present. The actual version of the CTRN is nevertheless the most precise document available and suitable for a large scale analysis. Despite this, it should be noticed that the roof surface computation is not based on samples, but on the whole cartographic database of the region. The extrapolated roof surface can be thus assumed to be errorless. The error due to the association building/municipality discussed in paragraph 2.2 *Territorial analysis* instead, has been estimated considering the municipality with the highest and lowest number of total buildings (respectively Torino and Claviere). Excluding the ambiguous buildings (falling on the administrative limit), thus associating to the relative municipality only the buildings falling completely within the administrative limits, gives a maximum relative error of 1.7%. The evaluation of the roof surface available, directly depends on the values assumed for the corrective coefficients (eq. 1), thus the variation of the coefficients affects directly the resulting PV potential. One may object on the arbitrariness of the empirical coefficients, however this approach represent a first tentative to address the lack of detailed informations on the roofing characteristics. The authors are currently working on an innovative methodology to eliminate the arbitrariness of this part of the methodology. The novel approach, based on the systematical image processing of ortho-images, will integrate

the present methodology and refine the computation of the coefficients.

The PV potential has been calculated assuming a mean solar radiation value in each municipality. Considering to assume the maximum and minimum value instead, yields a confidence level of ± 1% on the PV potential. The yearly PV energy yield per square meter of installation obtained (ranging between 65 and 161 $kWh/m^2 year$) is consistent with the results obtained by a similar work for Spain (Izquierdo et al., [6]).

5. Conclusions and developments

In the present paper, a methodology for the PV solar energy potential assessment has been presented. The hierarchical procedure proposed is accomplished through the evaluation of the useful global solar radiation, the roof surface available for roof-top integrated PV systems and their relative performances. Basically the procedure requires easy and freely accessible data, as solar radiation maps (database for Europe, [17]), statistical data on population and energy consumption and GIS data of the area object of study. It is indeed reproducible for other regions or countries at different scale (obviously depending on the computational resources available).

In the present work the methodology has been applied to the Piedmont Region (North-Western Italy). Different exploitation scenarios have been presented and it has been shown that, by means of roof-top integrated PV systems, the solar energy potential over the region may reach 6.9 TWh/year (according to the best exploitation scenario). It is interesting to denote that in 2009 the total net electrical energy consumption of the region has been of 24.5 TWh ca. (national net consumption of 300 TWh ca.) [9].

The presented methodology has been here applied for the PV solar energy potential assessment, but it can be easily applied for the solar-thermal potential assessment. For example, an interesting analysis could be the evaluation of the combined installation of PV and solar thermal systems, to achieve a totally *green strategy* in the distributed solar energy exploitation (see for instance Izquierdo et al., [24]), or for Solar Hydro-Electric systems (Glasnovic and Margeta, [25]).

Acknowledgments

References

[1] Conto Energia 2010. GSE S.p.a., Gestore Servizi Energetici. Publicly-owned company promoting and supporting renewable energy sources (RES) in Italy. 2010, (www.gse.it).

[2] Regional Council of Piedmont. 2010, (www.regione.piemonte.it).

[3] Castro M., Delgado A., Argul F., Colmenar A., Yeves F., Peire J., *Grid-connected PV buildings: analysis of future scenarios with an example of southern Spain*, Solar Energy 79 (2005) 8695.

[4] Sorensen B., *GIS management of solar resource data*, Solar Energy Materials and Solar Cells, 67 (2001)(14), 503509.

[5] EEA, 2010. European Environment Agency (http://www.eea.europa.eu/data-and-maps/).

[6] Izquierdo S., Rodrigues M., Fueyo N., *A method for estimating the geographical distribution of the available roof surface area for large-scale photovoltaic energy-potential evaluations*, Solar Energy 82 (2008) 92939.

[7] Kabir Md.H., Endlicher W., Jgermeyr J., *Calculation of bright roof-tops for solar PV applications in Dhaka Megacity, Bangladesh*, Renewable Energy 35 (8) (2010), pp. 1760-1764.

[8] Wiginton L.K., Nguyen H.T., Pearce J.M., *Quantifying rooftop solar photovoltaic potential for regional renewable energy policy*, Computers, Environment and Urban Systems 34 (4) (2010), pp. 345-357.

[9] Terna S.p.a., 2010. Energy Transmission Grid Operator. *Statistical Data on electricity in Italy (for 2009)*, (www.terna.it).

[10] GSE S.p.a., 2010. Gestore Servizi Energetici. Publicly-owned company promoting and supporting renewable energy sources (RES) in Italy. *Statistical Data on photovoltaic solar energy in Italy for 2009*, (www.gse.it).

[11] Šúri M., Huld T., Cebecauer T., Dunlop E.D., *Geographic Aspects of Photovoltaics in Europe: Contribution of the PVGIS Website*, IEEE Journal of Selected Topics in Applied Earth Observations and Remote Sensing, v 1, n 1, p 34-41, 2008.

[12] Šúri M., Hofierka J., *A new GIS-based solar radiation model and its application to photovoltaic assessments*, Transactions in GIS 8, 175190, 2004.

[13] Šúri M., Dunlop E.D., Huld T.A., 2005. *PV-GIS: A web based solar radiation database for the calculation of PV potential in Europe*, International Journal of Sustainable Energy 24 (2), 5567.

[14] Šúri M., Huld T., Cebecauer T., Dunlop E.D., Ossenbrink H.A., *Potential of solar electricity generation in the European Union*

member states and candidate countries, Solar Energy 81 (2007) 12951305.

[15] Lorenzo E., *Solar Electricity. Engineering of photovoltaic systems*, Progensa, 1994.

[16] ESRA, 2010. European Solar Radiation Atlas (http://www.helioclim.org/esra/).

[17] JRC, 2010. Joint Research Centre of the European Commission, IE Institute for Energy. *PVGIS*, (http://re.jrc.ec.europa.eu/pvgis/).

[18] ISTAT 2010. National Institute for Statistics, (www.istat.it).

[19] ISTAT 2010. National Institute for Statistics, (www.istat.it/strumenti/definizioni/comuni/).

[20] Skoplaki E., Palyvos J.A., *On the temperature dependence of photovoltaic module electrical performance: A review of efficiency/power correlations*, Solar Energy 83 (2009) 614624.

[21] Huld T., Gottschalg R., Beyer H.G., Topic M., *Mapping the performance of PV modules, effects of module type and data averaging*, Solar Energy 84 (2010) 324338.

[22] Carr A.J., Pryor T.L., *A comparison of the performance of different PV module types in temperate climates*, Solar Energy 76 (2004) 285294.

[23] UNI 10349, 1994.

[24] Izquierdo S., Montanés M., Dopazo, C., Fueyo N., *Roof-top solar energy potential under performance-based building energy codes: the case of Spain*, Solar Energy (2010) (in press).

[25] Glasnovic Z., Margeta J., *Sustainable Electric Power System, Is It Possible? - Case Study Croatia*, ASCE Journal of Energy Engineering 136 (2010) 103-113.

Table 5: Summary table for municipalities: Surface (S_{mun}) [km^2], Population (P_{mun}), population density (D_{pop}^{mun}) [$inhab/km^2$], number of residential buildings (N_{res}^{bui}), residential roof surface available (S_{res}^{avail}) [m^2], number of industrial buildings (N_{ind}^{bui}), industrial roof surface available (S_{ind}^{avail}) [m^2], total roof surface available (S_{tot}^{avail}) [m^2], mean solar radiation (H_m) [kWh/m^2year], PV potential for scenario A (res, ind, tot), (Π_A) [$GWh/year$].

Municipality	Prov.	S_{mun} $\left[km^2\right]$	P_{mun} $[-]$	D_{pop}^{mun} $\left[\frac{inhab}{km^2}\right]$	N_{res}^{bui} $[-]$	S_{res}^{avail} $\left[m^2\right]$	N_{ind}^{bui} $[-]$	S_{ind}^{avail} $\left[m^2\right]$	S_{tot}^{avail} $\left[m^2\right]$	H_m $\left[\frac{kWh}{m^2 year}\right]$	Π_A^{res} $\left[\frac{GWh}{year}\right]$	Π_A^{ind} $\left[\frac{GWh}{year}\right]$	Π_A^{tot} $\left[\frac{GWh}{year}\right]$
Almese	TO	17.9	6292	351	1849	25801	63	23089	48890	1622	3.578	3.202	6.780
Alpignano	TO	12.0	17246	1443	2330	40453	168	78753	119205	1587	5.491	10.689	16.180
Avigliana	TO	23.3	12183	524	2548	37188	93	27205	64393	1631	5.186	3.794	8.980
Beinasco	TO	6.8	18142	2684	1140	31082	154	184362	215444	1582	4.206	24.950	29.156
Borgaro Torinese	TO	14.4	13552	944	979	28337	150	114129	142465	1557	3.773	15.198	18.971
Brandizzo	TO	6.4	8141	1270	1272	24509	44	32953	57463	1563	3.275	4.404	7.679
Bruino	TO	5.6	8437	1509	1141	22518	105	62307	84825	1618	3.116	8.622	11.738
Bussoleno	TO	37.4	6597	176	2598	24990	106	22346	47336	1729	3.696	3.305	7.001
Buttigliera Alta	TO	8.3	6574	797	1157	18723	30	28901	47624	1611	2.579	3.981	6.560
Caluso	TO	39.5	7549	191	1418	51907	108	58092	110000	1547	6.866	7.685	14.551
Cambiano	TO	14.2	6318	444	889	18462	119	70318	88780	1595	2.519	9.592	12.111
Candiolo	TO	11.9	5646	474	741	19219	21	34004	53224	1591	2.615	4.627	7.242
Carignano	TO	50.2	9129	182	1645	52105	74	36114	88219	1591	7.090	4.914	12.004
Carmagnola	TO	96.4	27927	290	4777	94801	273	193842	288643	1611	13.062	26.708	39.770
Caselle Torinese	TO	28.7	17949	626	1937	52635	155	146309	198944	1554	6.993	19.439	26.433
Castellamonte	TO	38.5	9935	258	4346	73387	109	52876	126263	1565	9.823	7.077	16.900
Castiglione Torinese	TO	14.2	6261	442	1427	21416	41	12275	33691	1569	2.874	1.647	4.521
Cavour	TO	49.1	5592	114	2157	43473	93	32752	76225	1655	6.153	4.636	10.789
Chieri	TO	54.3	35849	660	4008	110565	300	169020	279584	1599	15.116	23.107	38.223
Chivasso	TO	51.3	25378	495	3233	80374	227	106262	186636	1547	10.634	14.059	24.694
Cirié	TO	17.8	18827	1058	2944	84348	129	110091	194440	1559	11.243	14.674	25.917
Collegno	TO	18.1	50072	2763	2977	62326	277	222485	284811	1573	8.382	29.922	38.304
Cumiana	TO	60.8	7858	129	2543	44416	61	26450	70865	1679	6.376	3.797	10.174
Cuorgné	TO	19.4	10175	525	2198	41078	67	33146	74224	1580	5.551	4.479	10.030
Druento	TO	27.7	8429	305	1196	24361	111	58964	83325	1562	3.253	7.875	11.128
Favria	TO	14.9	5148	347	1080	23453	99	36962	60415	1545	3.099	4.884	7.983
Gassino Torinese	TO	20.5	9578	468	1384	27733	25	10917	38650	1583	3.754	1.478	5.232
Giaveno	TO	72.0	16425	228	5146	68827	175	48287	117114	1714	10.087	7.076	17.163
Grugliasco	TO	13.1	37691	2873	2903	67478	332	316752	384230	1581	9.121	42.817	51.938
Ivrea	TO	30.2	24409	809	3303	77899	151	142606	220505	1517	10.104	18.496	28.600
La Loggia	TO	12.8	7666	599	1017	25764	57	99453	125217	1587	3.496	13.494	16.990
Lanzo Torinese	TO	10.4	5377	519	2047	32361	71	28071	60432	1597	4.420	3.834	8.254
Leiní	TO	32.5	14624	451	1910	57516	285	244160	301675	1555	7.649	32.472	40.121
Luserna San Giovanni	TO	17.7	7748	437	1721	33662	33	39958	73620	1724	4.962	5.890	10.852
Moncalieri	TO	47.6	57788	1213	5452	160633	300	324882	485514	1588	21.821	44.133	65.954
Montanaro	TO	20.8	5456	262	1092	24888	40	19273	44161	1548	3.295	2.552	5.847

Municipality	Prov.	S_{mun} $\left[km^2\right]$	P $[-]$	D_{pop} $\left[\frac{inhab}{km^2}\right]$	N_{res}^{bui} $[-]$	S_{res}^{avail} $\left[m^2\right]$	N_{res}^{bui} $[-]$	S_{res}^{avail} $\left[m^2\right]$	S_{tot}^{avail} $\left[m^2\right]$	H_m $\left[\frac{kWh}{m^2 year}\right]$	Π_A^{res} $\left[\frac{GWh}{year}\right]$	Π_A^{ind} $\left[\frac{GWh}{year}\right]$	Π_A^{tot} $\left[\frac{GWh}{year}\right]$
Nichelino	TO	20.6	49060	2377	2904	83173	175	168829	252002	1585	11.277	22.891	34.168
Nole	TO	11.3	6828	604	1378	27534	34	24465	52000	1563	3.681	3.271	6.952
None	TO	24.7	7927	321	1186	34822	77	114760	149582	1597	4.757	15.678	20.435
Orbassano	TO	22.1	22254	1009	1909	53470	231	176300	229770	1586	7.252	23.910	31.162
Pianezza	TO	16.5	13590	824	1741	34651	205	99378	134030	1565	4.637	13.297	17.934
Pinerolo	TO	50.3	35491	706	3833	105787	127	91298	197085	1687	15.266	13.175	28.440
Pino Torinese	TO	21.9	8663	396	1656	40176	13	3670	43846	1594	5.477	0.500	5.977
Piossasco	TO	40.0	18032	451	2070	46914	70	53139	100053	1632	6.547	7.416	13.964
Novara	NO	103.0	103602	1006	7324	240861	464	403427	644288	1501	30.912	51.775	82.687
Oleggio	NO	37.8	13222	350	2861	53126	162	73469	126595	1489	6.764	9.354	16.117
Poirino	TO	75.7	10149	134	2037	66157	161	123512	189669	1604	9.073	16.939	26.012
Rivalta di Torino	TO	25.3	19001	753	2391	55621	181	168505	224125	1605	7.635	23.131	30.766
Rivarolo Canavese	TO	32.3	12372	383	2152	53005	215	117633	170638	1545	7.004	15.544	22.548
Rivoli	TO	29.5	50015	1694	5626	105218	581	318699	423917	1595	14.351	43.468	57.819
San Benigno Canavese	TO	22.2	5577	251	1239	28132	65	29592	57725	1547	3.722	3.915	7.636
San Maurizio Canavese	TO	17.5	9123	521	1818	46732	71	50902	97634	1550	6.195	6.748	12.943
San Mauro Torinese	TO	12.6	19333	1540	1985	36447	167	175850	212296	1576	4.913	23.703	28.615
Santena	TO	16.2	10548	651	1733	37306	98	64793	102099	1595	5.089	8.839	13.928
Settimo Torinese	TO	32.4	47539	1469	3463	77858	419	453572	531431	1557	10.370	60.413	70.783
Strambino	TO	22.8	6381	280	1397	34623	62	32226	66849	1522	4.507	4.195	8.702
Susa	TO	11.3	6806	604	1997	23790	129	21782	45572	1668	3.393	3.106	6.499
Torino	TO	130.2	908825	6982	18843	1200464	1730	2572572	3773036	1576	161.810	346.755	508.565
Trofarello	TO	12.3	11125	903	1380	29753	114	73002	102755	1593	4.052	9.943	13.995
Venaria Reale	TO	20.3	34682	1709	1324	45444	169	179058	224502	1555	6.044	23.814	29.857
Vigone	TO	41.1	5300	129	1579	34538	156	52041	86578	1628	4.810	7.247	12.057
Vinovo	TO	17.7	13860	785	1817	50497	86	100595	151092	1586	6.850	13.645	20.495
Volpiano	TO	32.4	14771	456	3012	61174	188	130453	191627	1554	8.129	17.336	25.465
Volvera	TO	20.9	8643	413	1050	25652	67	84362	110014	1608	3.527	11.598	15.125
Borgosesia	VC	40.6	13447	332	2624	50847	96	92698	143546	1518	6.600	12.033	18.633
Crescentino	VC	48.3	8124	168	1368	44551	54	73768	118318	1542	5.875	9.729	15.604
Gattinara	VC	33.5	8399	250	1314	35562	84	89789	125351	1496	4.549	11.484	16.033
Santhiá	VC	53.3	9078	170	1616	35785	155	76576	112361	1507	4.611	9.867	14.478
Serravalle Sesia	VC	20.4	5129	252	1066	24199	77	60955	85154	1505	3.115	7.847	10.963
Trino	VC	70.6	7711	109	1140	47056	87	78010	125066	1530	6.158	10.209	16.368
Varallo	VC	88.7	7586	86	2277	38368	40	23737	62106	1530	5.020	3.106	8.126
Vercelli	VC	79.8	47080	590	3774	136514	344	281598	418113	1513	17.665	36.439	54.104
Arona	NO	14.9	14588	980	2117	47560	54	30641	78201	1480	6.021	3.879	9.901
Bellinzago Novarese	NO	39.3	9120	232	1614	36050	52	27760	63811	1493	4.602	3.544	8.145
Borgomanero	NO	32.3	21305	660	4177	76976	182	92406	169382	1495	9.841	11.814	21.655
Cameri	NO	39.6	10792	272	1619	31189	91	73363	104552	1496	3.990	9.385	13.375
Castelletto sopra Ticino	NO	14.6	10000	686	2109	41377	66	34521	75898	1476	5.222	4.356	9.578
Cerano	NO	32.1	6879	214	944	32113	84	67261	99374	1499	4.116	8.620	12.736

Municipality	Prov.	S_{mun} $\left[km^2\right]$	P [-]	D_{pop} $\left[\frac{inhab}{km^2}\right]$	N_{res}^{bui} [-]	S_{res}^{avail} $\left[m^2\right]$	N_{ind}^{bui} [-]	S_{ind}^{avail} $\left[m^2\right]$	S_{tot}^{avail} $\left[m^2\right]$	H_m $\left[\frac{kWh}{m^2 year}\right]$	Π_A^{res} $\left[\frac{GWh}{year}\right]$	Π_A^{ind} $\left[\frac{GWh}{year}\right]$	Π_A^{tot} $\left[\frac{GWh}{year}\right]$
Galliate	NO	29.5	15062	510	2052	54012	135	85795	139807	1496	6.908	10.974	17.882
Gozzano	NO	12.5	5808	464	1510	27748	109	70643	98391	1503	3.568	9.082	12.650
Romentino	NO	17.7	5133	290	675	19808	40	23820	43628	1496	2.534	3.048	5.582
Trecate	NO	38.4	19602	511	1804	48090	147	84707	132797	1499	6.166	10.862	17.028
Alba	CN	54.0	30994	574	3505	101333	118	167527	268860	1632	14.140	23.376	37.516
Bagnolo Piemonte	CN	62.9	5969	95	3008	47984	11	7614	55598	1713	7.030	1.116	8.146
Barge	CN	82.4	7757	94	3874	62643	74	26864	89506	1692	9.064	3.887	12.951
Borgo San Dalmazzo	CN	22.3	12212	549	1856	42916	93	68995	111911	1781	6.538	10.511	17.049
Boves	CN	51.1	9889	194	2305	47134	38	32946	80080	1777	7.163	5.007	12.169
Bra	CN	59.6	29608	497	4462	106266	201	160320	266586	1633	14.837	22.384	37.221
Busca	CN	65.8	9941	151	2748	64816	86	43673	108490	1743	9.662	6.510	16.173
Canale	CN	18.0	5747	319	1200	29987	59	42219	72206	1615	4.141	5.830	9.970
Caraglio	CN	41.5	6780	163	1933	42321	59	29568	71889	1776	6.427	4.491	10.918
Cavallermaggiore	CN	51.6	5418	105	1340	40609	70	42846	83455	1634	5.675	5.988	11.663
Centallo	CN	42.8	6681	156	1607	40274	38	19013	59287	1713	5.901	2.786	8.687
Ceva	CN	43.0	5884	137	1373	33042	31	21064	54106	1691	4.779	3.046	7.825
Cherasco	CN	81.2	8287	102	2132	56533	128	107956	164489	1639	7.922	15.128	23.051
Cuneo	CN	119.9	55201	460	5955	207519	240	251439	458957	1752	31.101	37.683	68.784
Dronero	CN	58.9	7313	124	2108	48223	37	30131	78353	1772	7.308	4.566	11.875
Fossano	CN	130.7	24595	188	4568	124739	236	181887	306626	1685	17.974	26.208	44.182
Mondoví	CN	87.3	22473	258	3562	98159	180	146642	244801	1707	14.326	21.403	35.729
Peveragno	CN	68.4	5448	80	2214	49593	31	22365	71959	1775	7.528	3.395	10.923
Racconigi	CN	48.0	10068	210	1746	48866	87	63144	112010	1621	6.773	8.752	15.526
Saluzzo	CN	75.8	16797	222	2575	83676	95	70236	153912	1657	11.857	9.953	21.810
Savigliano	CN	110.7	20845	188	3215	111334	211	130787	242121	1664	15.845	18.613	34.458
Sommariva del Bosco	CN	35.6	6326	178	1294	33520	43	33798	67317	1625	4.658	4.697	9.354
Verzuolo	CN	26.2	6406	245	1312	34226	34	57965	92191	1701	4.979	8.433	13.412
Villanova Mondoví	CN	28.4	5771	203	1405	32452	51	26498	58951	1742	4.835	3.948	8.783
Asti	AT	151.8	75298	496	10530	195098	816	378624	573722	1580	26.356	51.148	77.503
Canelli	AT	23.6	10628	451	2213	57366	178	131182	188547	1595	7.823	17.889	25.713
Costigliole d'Asti	AT	36.9	6061	164	2404	45872	102	30630	76502	1595	6.258	4.178	10.436
Nizza Monferrato	AT	30.4	10388	342	2173	57570	119	54218	111788	1587	7.816	7.361	15.176
San Damiano d'Asti	AT	48.0	8445	176	2602	49279	132	43608	92887	1597	6.731	5.956	12.687
Villanova d'Asti	AT	42.1	5600	133	1448	37045	140	133000	170045	1607	5.090	18.274	23.364
Acqui Terme	AL	33.4	20426	611	3059	75170	108	62722	137892	1589	10.216	8.524	18.740
Alessandria	AL	204.0	93676	459	10617	300326	643	426932	727258	1537	39.485	56.131	95.616
Arquata Scrivia	AL	23.4	6127	262	1538	21886	38	46195	68081	1588	2.973	6.275	9.248
Casale Monferrato	AL	86.3	36039	418	4429	163582	188	172619	336201	1532	21.428	22.612	44.040
Castelnuovo Scrivia	AL	45.4	5513	121	1023	38368	65	43677	82044	1517	4.977	5.666	10.642
Novi Ligure	AL	54.2	28581	527	3476	85134	123	110296	195430	1562	11.375	14.737	26.112
Ovada	AL	35.3	11912	337	2047	48721	76	74640	123360	1607	6.695	10.257	16.953
Serravalle Scrivia	AL	16.0	6272	392	1113	21716	60	69499	91215	1566	2.908	9.308	12.217

Municipality	Prov.	S_{mun} $[km^2]$	P $[-]$	D_{pop} $\left[\frac{inhab}{km^2}\right]$	N_{res}^{bui} $[-]$	S_{res}^{avail} $[m^2]$	N_{res}^{bui} $[-]$	S_{res}^{avail} $[m^2]$	S_{tot}^{avail} $[m^2]$	H_m $\left[\frac{kWh}{m^2 year}\right]$	Π_A^{res} $\left[\frac{GWh}{year}\right]$	Π_A^{ind} $\left[\frac{GWh}{year}\right]$	Π_A^{tot} $\left[\frac{GWh}{year}\right]$
Tortona	AL	99.3	27476	277	4004	96704	390	262833	359537	1534	12.684	34.474	47.158
Valenza	AL	50.1	20282	405	2247	69064	55	30661	99726	1531	9.045	4.015	13.060
Domodossola	VB	36.9	18452	501	3357	63174	51	33921	97095	1489	8.047	4.321	12.368
Biella	BI	46.7	45842	982	4605	107990	366	280429	388419	1503	13.884	36.054	49.938
Candelo	BI	15.1	8041	534	1445	32680	45	35971	68651	1489	4.160	4.579	8.740
Cossato	BI	27.8	15050	542	3146	51316	163	111653	162969	1496	6.567	14.288	20.855
Trivero	BI	29.9	6326	212	1475	27997	69	101319	129315	1515	3.628	13.128	16.756
Vigliano Biellese	BI	8.4	8482	1012	1532	24279	116	93399	117678	1489	3.091	11.890	14.981
Cannobio	VB	51.2	5132	100	1465	28206	12	1784	29990	1453	3.505	0.222	3.726
Gravellona Toce	VB	14.7	7781	529	1255	21765	95	66998	88762	1469	2.734	8.416	11.149
Omegna	VB	30.8	16074	522	2802	52550	166	109813	162363	1500	6.739	14.083	20.823
Stresa	VB	33.2	5179	156	2060	33041	7	2780	35821	1453	4.106	0.345	4.451
Verbania	VB	37.7	31134	827	4283	81888	177	114607	196494	1441	10.091	14.123	24.213
Villadossola	VB	18.0	6909	385	1665	22646	77	60837	83483	1471	2.849	7.653	10.501